RSC Advances

PAPER

View Article Online
View Journal | View Issue

Cite this: *RSC Adv.*, 2019, **9**, 41280

Amphiphilic copolymer self-assembly of magnetic nanoparticles for construction of magnetically responsive photonic crystals based on steric hindrance†

Meng Shang, Xinjiong Ni, Jiasheng Xu and Yuhua Cao *

Herein, a facile, simple and rapid self-assembly of magnetic colloidal nanoparticles (MCNPs) to build magnetically responsive photonic crystals (MRPCs) was devolved. A nonionic amphiphilic random copolymer poly(styrene-*co*-vinylpyrrolidone) P(St-*co*-VP) with the monomer molar ratio of 1 : 9 was used not only as an emulsifier for miniemulsion self-assembly of Fe_3O_4 magnetic nanoclusters, but also as the coating material on the magnetic nanoclusters through itself assembly. The self-assembly of the magnetic nanocluster and the polymer coating were completed simultaneously without another polymerization process. The characterization of the MCNPs and the optical properties of the MRPCs were investigated in details. TEM showed that the MCNPs had regular spherical structures with an average diameter of 104.6 nm (RSD = 13.9%, $n = 100$). P(St-*co*-VP) self-assembly coating was confirmed by IR and XPS, and thermogravimetric analysis showed that the magnetite content was 76.15%. The large content of magnetite and the thin coating of the copolymer gave MCNPs the high saturated magnetization (M_s) of 52.60 emu g^{-1}. Under an external magnetic field, the MCNPs could assemble MRPCs instantaneously and reversibly. The structural color covered entire visible spectrum by tuning the strength of the external magnetic field. On basis of the steric hindrance from neighboring PVP stretching chains, rather than electrostatic repulsion or solvation layer to counterbalance magnetic attraction, the MRPCs could tolerate the electrolyte as high as 0.10 mol L^{-1} and the variance of pH from 2.0–12.0. The stability of P(St-*co*-VP) self-assembly coating was testified through the invariability of the structural color of MRPCs after repeated washing, as well as the recovery of structural color after removing the electrolytes.

Received 31st October 2019
Accepted 2nd December 2019

DOI: 10.1039/c9ra08962d

rsc.li/rsc-advances

Introduction

Photonic crystals (PCs) are periodic nanostructures consisting of two or more materials with different dielectric constants. PCs exhibit photonic band gap (PBG), which prohibits light propagation in certain wavelength and give PCs unique structural color characteristics. PBG enables PCs to manipulate photons, just as electronic bandgap makes semiconductor to control electrons. Due to their unique structures and properties, PCs show the great potentials in display devices,[1] eco-friendly printings and paintings,[2] anti-counterfeiting technologies,[3,4] chemical and biological sensors.[5] The fabrication of PCs can be divided into "up-to-bottom"[6] and "bottom-to-up".[7] "Bottom-to-up" strategy is self-assembly of monodisperse colloidal particles driven by external forces, such as gravity, centrifugal force, capillary force, electric field, magnetic field, *etc.* Among them, the magnetic assembly is controllable, rapid and reversible, and has aroused the interest of the scientists.[8]

MRPCs are composed of MCNPs, which are spatially ordered under the external magnetic field on basis of the balance between the magnetic attraction and repulsive force among the adjacent particles. In general, MCNPs are obtained by preparing nanoclusters of superparamagnetic ferrites through solvothermal method to obtain high M_s.[9–11] The subsequent coating on the nanoclusters is indispensable, not only to avoid the agglomeration owing to the ferromagnetic effect of supercritical size on the premise of maintaining the appropriate size morphology,[12] but also to provide the corresponding repulsive force such as electrostatic repulsion, solvation layer or steric hindrance for assembly of MRPCs. Xu *et al.* prepared superparamagnetic monodisperse Fe_3O_4@PS nanospheres by emulsion polymerization for the first time.[13] However, the magnetite content of the nanosphere was only 17%, and the PBG regulated by the external magnetic field was narrow. In order to improve the content of the magnetic materials, Ge *et al.* prepared superparamagnetic colloidal nanocrystals by hydrothermal method, then polyacrylic acid (PAA) was coated.[14] The MCNPs

School of Chemical and Material Engineering, Jiangnan University, Wuxi, 214122, People's Republic of China. E-mail: yuhuacao64@gmail.com

† Electronic supplementary information (ESI) available. See DOI: 10.1039/c9ra08962d

had high M_s and large specific surface charge density, and the PBG covered the entire visible region. However, the electrostatic repulsion from PAA coatings was susceptible to the surrounding environment such as ion concentration, pH and solvent, which led to structure color blue-shifted, red-shifted or even vanished. Subsequently, Ge *et al.* used the Stöber method to coat the SiO_2 on the surface of magnetic nanoclusters.[15] It stabilized MRPCs through the solvation layer generated by hydrogen bonding, and realized the magnetic responsiveness of the MRPCs in organic solvents. However, the tunable range of the PBGs was narrow. Recently, Luo *et al.* synthesized superparamagnetic Fe_3O_4@PVP colloidal particles by solvothermal method with high M_s of 53.5 emu g^{-1}.[16] The MRPCs were constructed by the long-range steric repulsion provided by the nonionic polymer polyvinylpyrrolidone (PVP), rather than electrostatic repulsion. Therefore, they would be substantially unsusceptible to ionic strength, pH and solvent polarity. The MRPCs structural color in polar solvents (such as *N*,*N*-dimethylformamide) could cover the entire visible spectrum by adjusting external magnetic field, which further expanded the application field of MRPCs. However, a high temperature and pressure environment, a specific reaction vessel and the long reaction time were essential for solvothermal synthesis of Fe_3O_4@PVP colloidal particles. Therefore, a simple, rapid and controllable preparation of MCNPs with high M_s and anti-environmental interference is imperative in the research of MRPCs.

In our previous work, MCNPs with core–shell structures had obtained through miniemulsion assembly of magnetic nanoclusters as the core, followed by miniemulsion polymerization of polymer shell.[17] Miniemulsion refers to a stable dispersion of submicron (50–500 nm) oil-in-water droplets formed by the synergistic action of the emulsifier and the co-emulsifier under high shear or ultrasonic conditions.[18] The droplet size is between the microemulsion (less than 100 nm) and the emulsion (micron). Micellar nucleation in emulsion polymerization can be avoided by controlling the surfactant concentration below the critical micelle concentration (CMC).[19] The miniemulsion droplet acts as a "micro-reactor", where the polymerization reaction takes place. Therefore, the size of the product would be located in submicron level, which is just right for construction of PCs with PBG in visible spectrum. Miniemulsion polymerization is considered to be the most effective method for preparing MCNPs.[20–22] In our previous work, it was found that the size and M_s of MCNPs were controllable by conveniently adjusting the amount of an emulsifier SDS.

Herein, we prepared MCNPs through the miniemulsion self-assembly by an amphiphilic copolymer with one-step process, without additional polymerization reaction. An amphiphilic random copolymer was used not only as the emulsifier for formation miniemulsion, but also as MCNPs coating material by itself assembly. The whole procedures to form MRPCs were interpreted in Scheme 1. The developed method is faster, simpler, more convenient and easier to control.

A nonionic amphiphilic random copolymer P(St-*co*-VP) with the monomer molar ratio of 1 : 9 was chosen in the present work for three reasons. Firstly, P(St-*co*-VP) (1 : 9) was an excellent emulsifier to form dispersible and stable oil-in-water

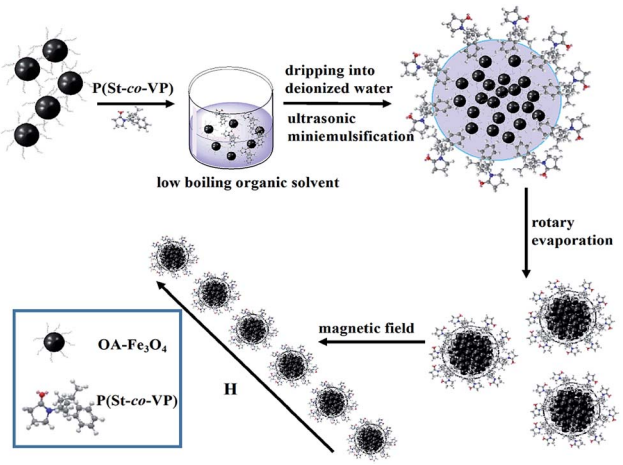

Scheme 1 Schematic diagram of the procedure for the preparation of MCNPs and MRPCs.

miniemulsion droplets in miniemulsion system. The oil droplet consisting of oleate modified Fe_3O_4 nanoparticles and chloroform was stabilized in aqueous phase by the amphiphilic polymer P(St-*co*-VP), where hydrophobic moieties PS inserted in oil phase, and hydrophilic PVP stretched outward in aqueous phase. Secondly, during chloroform evaporation, magnetic nanocluster formed and P(St-*co*-VP) self-assembled on the surface of nanoclusters to form aggregates as the coating materials. The coordination effect between iron and PVP made the P(St-*co*-VP) coatings fixated, which suffered from washing process. Lastly, the hydrophilic chain PVP stretched outward, not only as the MCNPs protective layers, but also as steric hindrance to balance the magnetic attraction under magnetic assembly of MRPCs. The assembly mechanism avoided the influences of ion strength and pH of surrounding environment. The formation of magnetic nanoclusters and the self-assembly coating of amphiphilic random copolymer are accomplished simultaneously. The thin self-assembly coating was beneficial to enhancement of M_s of MCNPs. Thus, miniemulsion self-assembly using amphiphilic random copolymer as the emulsifier and coating materials to rapidly prepare MCNPs was studied in the present work.

Experimental section

Chemical

Styrene (St, AR), *N*-vinylpyrrolidone (N-VP, AR), azodiisobutyronitrile (AIBN, AR), *N*,*N*-dimethylformamide (DMF, AR), 1,4-dioxane (AR), anhydrous ether (AR), iron sulfate heptahydrate ($FeSO_4 \cdot 7H_2O$, AR), ferric trichloride hexahydrate ($FeCl_3 \cdot 6H_2O$, AR), ammonia ($NH_3 \cdot H_2O$, 25%, AR), oleic acid (OA, AR), anhydrous ethanol (AR), chloroform ($CHCl_3$, AR), sodium chloride (NaCl, AR), sodium hydroxide (NaOH, AR), hydrochloric acid (HCl, AR) were purchased from Sinopharm Chemical Reagent Co., Ltd. (China). All chemicals were used as received without further purification.

Preparation of the amphiphilic random copolymer P(St-*co*-VP)

St (0.01 mol) and N-VP (0.09 mol) were dissolved with 30 mL 1,4-dioxane in a 250 mL one-necked round-bottom flask, and the initiator AIBN, 3.0% of the total weight of the monomers, was added. After flushing nitrogen for 30 min, the round-bottom flask was sealed and the reaction happened under magnetic stirring in a 65 °C oil bath for 24 hours. After that, it was cooled to room temperature, and the crude product was precipitated with an appropriate amount of anhydrous ether. Then, the copolymer was purified by washing with anhydrous ether for three times. Finally, the product was dried in a vacuum oven at 45 °C overnight, and sealed at room temperature for storage.

The copolymer was characterized by Fourier transform infrared spectroscopy (FTIR) (WQF-600N, Beijing Rayleigh Analytical Instrument Co. Ltd., China), gel permeation chromatograph (GPC) (Waster, USA) and nuclear magnetic resonance spectroscopy (^{1}H NMR) (AVANCE III HD 400 MHz, Brook, Swiss), shown in ESI in details.† FTIR spectrum displayed PS (1600 cm^{-1}, 1492 cm^{-1}, 760 cm^{-1} and 700 cm^{-1}) and PVP (1680 cm^{-1} and 1283 cm^{-1}) characteristic absorption peaks in Fig. S1.† The molecular weight of P(St-*co*-VP) was 100 800 determined with GPC in Fig. S2.† From ^{1}H NMR in Fig. S3,† the molar ratio of St to VP was 1 : 10, close to the feed ratio of 1 : 9.

Preparation of the MCNPs

OA modified superparamagnetic Fe_3O_4 (OA-Fe_3O_4) nanoparticles were prepared following the modified chemical co-precipitation procedure.[23] Firstly, 100 mg OA-Fe_3O_4 and 360 mg P(St-*co*-VP) were dispersed in 4 mL chloroform as the oil phase. The well-dispersed oil phase was added in 36 mL deionized water, and miniemulsified for 2 min with 240 W Ultrasonic cell disruption system (JP-1200Y, Wuxi Jiuping Instrument Co. Ltd., China). Then, the miniemulsion was transferred to a one-necked round-bottom flask, and chloroform was evaporated by rotary evaporation using a rotary evaporator (RE-52C, Zhengzhou Kehua Instrument Equipment Co. Ltd., China) to obtain the MCNPs. Finally, the particles were washed repeatedly with deionized water until the conductivity was consistent with that of the deionized water (3.80 μs cm^{-1}, at 25 °C). The cleaned MCNPs were dispersed in deionized water and stored for use. The collection and washing of MCNPs was carried out with magnetic separation.

Construction of the MRPCs

The MCNPs were dispersed in deionized water, and were magnetically assembled instantaneously to obtain PCs with bright structural color using a permanent magnet (50 × 10 mm, Shanghai Xiefu Industrial Co. Ltd., China). By changing the magnetic field intensity (H) through adjusting the distance between the sample bottle and the magnet, the structural color of PCs could be tuned, and the optical properties of PCs were recorded with micro fiber spectrometer (FLA-5000+, Hangzhou Jingfei Technology Co., Ltd., China). The ability of MRPCs to resist environmental interference was investigated by changing the ionic strength and pH.

Results and discussion

Characterization of the MCNPs

Scheme 1 is a schematic diagram to interpret preparation of the MCNPs by the miniemulsion self-assembly method using an amphiphilic random copolymer P(St-*co*-VP). The MRPCs, using MCNPs as the building blocks, were constructed under an external magnetic field. The magnetic dipole–dipole force drives the self-assembly of particles into 1D chain-like structures along the external field.[24]

The transmission electron microscopy (TEM) (JEM-2100, JEOL, Japan) images of the MCNPs (a) and the MCNPs sample dried under the magnetic field (b and c) were shown in Fig. 1. It was found that the nanoparticles were almost uniform in size and had regular spherical shape. According to the random statistics of the particle sizes of 100 particles in the TEM images, the average particle size of the MCNPs was 104.6 nm (RSD = 13.9%). It indicated that the MCNPs were of monodispersity. Without a magnetic field, the MCNPs were disorderly dispersed, and there was a large distance between the nanoparticles, as shown in Fig. 1a. It revealed that copolymer coatings protected MCNPs well from the agglomeration. Under the external magnetic field, Fig. 1b clearly showed that the particles assembled into an ordered periodic chain structures. In particular, it could be seen from Fig. 1c that the Fe_3O_4 nanoclusters formed in the inner of MCNPs, but the polymer coating was too thin to be observed. The thin polymer coating and large magnetic nanocluster core were a decisive factor to obtain high M_s.[25]

Fig. 2a showed FTIR spectra of OA-Fe_3O_4 nanoparticles and MCNPs, respectively. The absorption peak at 578 cm^{-1} in both spectra was the characteristic absorption peak of Fe–O bond, which indicated that MCNPs contained Fe_3O_4 nanoparticles. The absorption peak at 1630 cm^{-1} was the characteristic absorption peak of C=O in oleate, which confirmed the carboxylate of oleate bonded to Fe_3O_4 through chelation. Besides, FTIR spectrum of the MCNPs had a strong absorption peak at 1665 cm^{-1}, which was ascribed to the stretching vibration C=O of PVP in P(St-*co*-VP). An additional absorption peak appeared at 1283 cm^{-1}, which was the characteristic absorption peak of the C–N bond of PVP in P(St-*co*-VP). The frame vibration of the benzene in P(St-*co*-VP) (1 : 9) was covered by C=O peak, nevertheless, C–H out-of-plane bending vibration of monosubstitute benzene in P(St-*co*-VP) had a strong absorption peak at 700 cm^{-1}. The FTIR spectrum of P(St-*co*-VP) (1 : 9) also showed the strong absorption peak at 700 cm^{-1}. Therefore,

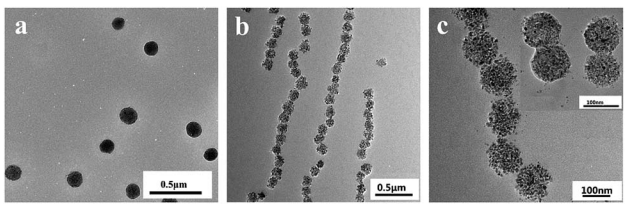

Fig. 1 TEM images of MCNPs (a) and MCNPs sample dried under magnetic field (b and c) on the double-carbon supporting film.

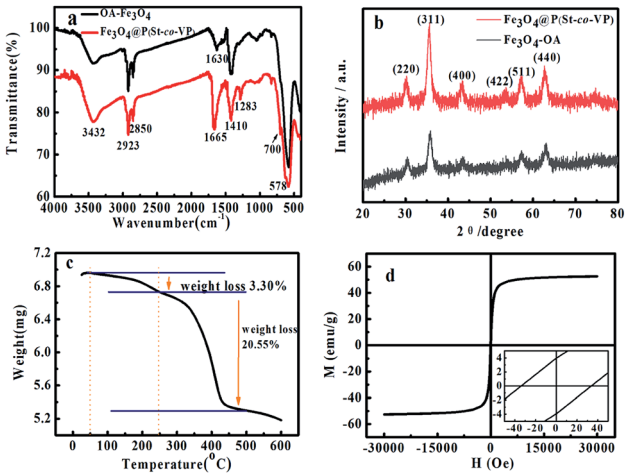

Fig. 2 (a) FTIR spectra of the OA-Fe_3O_4 particles and the MCNPs, (b) XRD patterns of the OA-Fe_3O_4 and the MCNPs, (c) TG curve of the MCNPs, (d) hysteresis loop of the MCNPs.

the FTIR spectra indicated that P(St-*co*-VP) was coated on the surface of MCNPs. OA-Fe_3O_4 nanoparticles and MCNPs was characterized by an X-ray diffraction analyzer (XRD) (Germany Brook AXS Co. Ltd., Germany). Fig. 2b showed the XRD pattern of OA-Fe_3O_4 nanoparticles and MCNPs. The diffraction peaks in two XRD spectra corresponded to the (220), (311), (400), (422), (511) and (440) crystal planes. Through the comparative analysis with standard diffraction card PDF26-1136, it was consistent with the characteristic diffraction peaks of the standard Fe_3O_4. It indicated that OA-Fe_3O_4 nanoparticles and the MCNPs were the cubic trans-spinel structure of Fe_3O_4. The diffraction peak shape of Fe_3O_4 was narrow and sharp, it revealed that the grain was intact and the degree of crystallization was good.

Fig. 2c was the thermogravimetric (TG) (TGA/DSC1/1100SF, Mettler Toledo International Trade Co. Ltd., Switzerland) curve of the MCNPs. TG curve showed a slowly decreasing trend in the range of 25–250 °C, and the weight loss was 3.30%. It was ascribed to the evaporation of the physical-chemical adsorbed water and traces of organics;[26] in the range of 250–500 °C, there was a sharp downward trend in TG curve and the weight loss was 20.55%. It is derived from the thermal decomposition of organic components in the MCNPs.[25] As the temperature continued to rise, TG curve became flat, indicating that the organic components had been burned out. The remaining mass was 76.15%, which belonged to ferromagnetic materials with high thermal stability (Fe_3O_4 or Fe_2O_3).[16] Therefore, the magnetite content in the MCNPs was 76.15%, 4 times as much as that in superparamagnetic Fe_3O_4@PS nanospheres.[13] This was consistent with the observation of the MCNPs in TEM.

Magnetic properties of MCNPs were measured with vibrating sample magnetometer (VSM) (MPMS XL-7, Quantum Design, USA) to obtain the hysteresis loop (Fig. 2d). It could be concluded from the hysteresis loop that the M_s of MCNPs was 52.60 emu g^{-1}. The M_s was much higher than M_s of superparamagnetic Fe_3O_4@PS nanospheres and Fe_3O_4@SiO_2 magnetic nanospheres reported previously,[13,15] and equivalent to M_s of the superparamagnetic Fe_3O_4@PAA and Fe_3O_4@PVP nanoparticles.[14,16] The higher M_s endowed the MCNPs with higher magnetic sensitivity and the more controllable assembly of MRPCs instantaneously. PVP has coordination interaction with Fe_3O_4. During self-assembly of amphiphilic random copolymer P(St-*co*-VP), the PVP drove Fe_3O_4 nanoparticles toward the periphery, which also increased the M_s of MCNPs. The coercive force (H_c) and remnant magnetization (M_r) of MCNPs was 33.95 Oe and 3.95 emu g^{-1}, respectively, shown in the enlarged scale view of Fig. 2d. Both H_c and M_r were not theoretically zero, which indicated that MCNPs were paramagnetic materials, close to superparamagnetism.

The surface element composition of the MCNPs was characterized by X-ray photoelectron spectroscopy (XPS) (Axis supra, Kratos, UK), shown in Fig. 3a. The results showed that the surface of the MCNPs contained 69.10% C, 20.48% O, 7.06% Fe and 3.36% N. XPS is a kind of surface analysis technique, which probes the outermost 5–10 nm thickness of the MCNPs.[27] Therefore, the surface of the MCNPs was comprised of a large of organic polymer P(St-*co*-VP) and a small part of Fe_3O_4. To determine the chemical state of each element, high resolution XPS spectra of N 1s, O 1s and Fe 2p were highlighted, as shown in Fig. 3b–d. In Fig. 3b, the fitting results of N 1s revealed that the particles surface had only one chemical state of N, the binding energy of N 1s was consistent with that in pure PVP.[27] In Fig. 3c, the O 1s line was fitted three peaks, 529.8 eV, 530.9 eV and 532.0 eV, corresponding to three different chemical states.[28,29] According to the relevant references, the first peak (529.8 eV) was matched with the binding energy of O from Fe_3O_4,[30] the second peak (530.9 eV) could be assigned to the free O in PVP,[27] while the last peak (532.0 eV) was attributed to O from PVP coordinating with the Fe_3O_4.[31] On the basis of this analysis, it was verified that PVP had coordination effect with Fe_3O_4, which made Fe_3O_4 nanoparticles appear at the periphery of the nanoparticles. In Fig. 3d, the peak of 710.4 eV and 724.2 eV was the binding energy of Fe $2p_{3/2}$ and Fe $2p_{1/2}$,

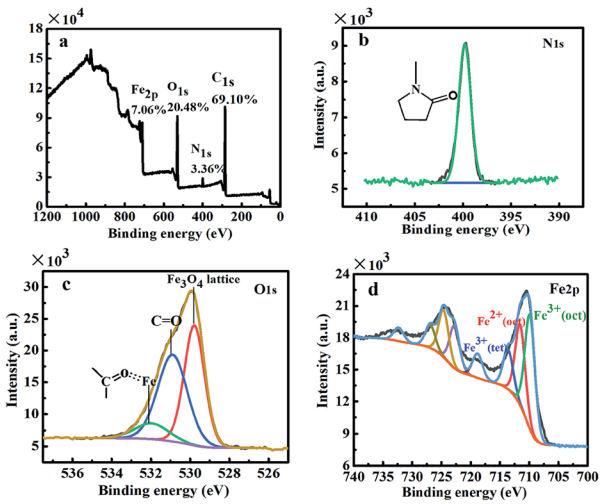

Fig. 3 (a) XPS spectra of the MCNPs and high-resolution XPS spectra of the MCNPs (b) N 1s, (c) O 1s and (d) Fe 2p.

respectively. The results were consistent with the typical characteristics of the XPS data of Fe_3O_4 reported in the literature.[32,33] The fitting results of Fe 2p showed that the molar ratio of octahedral and tetrahedral Fe^{3+} to octahedral Fe^{2+} was 1.90.[34,35] Therefore, during assembly process, Fe_3O_4 in MCNPs was not oxidized.

Optical properties of MRPCs

Magnetically responsive of the MCNPs. MCNPs with a concentration of 1.00 mg mL^{-1} were magnetically assembled into PCs in a magnetic field. Fig. 4a showed the reflection spectra of the MRPCs corresponding to different H, and Fig. 4b was an optical picture of the MRPCs corresponding to the different H. H could be adjusted by changing the distance between the magnet and the sample bottle. According to the Bragg diffraction equation $\lambda = 2nd \sin\theta$ (λ is the diffraction wavelength; n is the refractive index of water 1.33; d is the lattice plane spacing; θ is the Bragg angle 90°),[36–38] λ was proportional to d since n and θ were fixed. The lattice plane spacing d depends on the balance between magnetic attraction of Fe_3O_4 nanoclusters and long-range steric repulsion of PVP on the surface of MCNPs. An increase of H strengthened the magnetic attraction between the MCNPs. After rebalancing magnetic attraction and the long-range steric repulsion, the spacing between nanoparticles became shortened, which made λ blue-shifted. If H weakened, λ red-shifted reversely. The optical response of the MCNPs to the external magnetic field was instantaneous and fully reversible. The PBG had a wide adjustable range, which covered the entire visible spectrum. The tunable spectral range was wider than that of MRPCs made up of Fe_3O_4@PVP particles,[16] and the spectral reflection intensity was also higher. In addition, the required H for realizing the ordering of MCNPs and color tuning of MRPCs was typically in the range of 0.3–0.01 T. The research process used the rubidium ferroboron strong magnet, and the H of the disk-shaped magnet was measured by a handheld digital Tesla meter (TD8620, Changsha Tianheng Measurement and Control Technology Co. Ltd., China). Fig. 4b showed the H at the center of the disk-shaped magnet.

Anti-interference of the MRPCs. According to the classic Derjaguin–Landau–Overbeek–Verwey (DLOV) theory,[39] increasing the ionic strength of the aqueous solutions can largely compress the double electric layer and shield electrostatic forces. Therefore, when the concentration of NaCl increased to 1.0×10^{-2} mol L^{-1} or less, the MRPCs stabilized by the electrostatic repulsion would coagulate and lose the characteristics of PCs. It is due to the fact that the electric double layer become thinner and shields the electrostatic force. It is insufficient to resist the magnetic attraction, and finally the agglomeration of the magnetic nanoparticle occurs. In contrast, the MRPCs relied on PVP long-range steric repulsion stabilization, could remain stable at higher ionic strengths or at acidic and alkaline conditions.

Fig. 5 showed the reflection spectra of the MRPCs as NaCl concentration from 1.0×10^{-4} mol L^{-1} to 1.0×10^{-1} mol L^{-1} at pH 6.0–7.0. It could be seen that MCNPs remained stable and the diffraction peak of MRPCs covered entire visible spectra with the increase of H. On the other hand, though the structural color still remained, the diffraction peaks blue-shifted slightly and the strength of diffraction light weakened as NaCl concentration became 0.010 mol L^{-1} and 0.10 mol L^{-1}.

Fig. 6 showed the reflection spectra of the MRPCs as pH ranged from 2.0 to 12.0, adjusted by adding HCl or NaOH aqueous solution. The diffraction peak of the MRPCs still exhibited a wide tunable spectral range as the H increases. It indicated that the optical properties of the MRPCs were insensitive to the variance of pH because of non-ionic PVP polymer on the surface of MCNPs. The change of pH in a certain range had no significant effect on the surface charge density. However, if the acidity or alkalinity increased further, the structural color of MRPCs disappeared, and MCNPs gradually dissolved.

MRPCs based on steric-repulsion mechanism would tolerate the high concentration of the electrolytes, and the wide range of pH, which extremely extended MRPCs application.

Stability and reproducibility of the MRPCs. The stability of P(St-*co*-VP) assembly coatings on the MCNPs might be the most concerned problem. In order to dispel such concern, the MCNPs were washed with deionized water for 10 times, and the structural colors of the MRPCs remained unchanged, as shown in Fig. 7. It indicated that the assembly coatings could be firmly

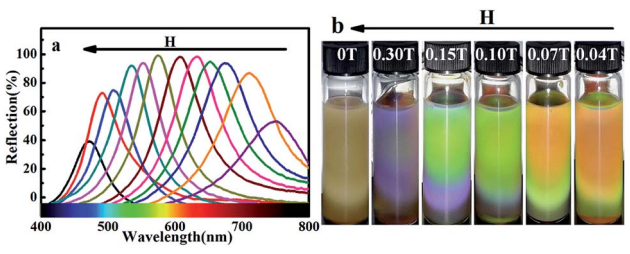

Fig. 4 (a) Reflection spectra of the MRPCs corresponding to different magnetic field strength H, (b) optical pictures of the MRPCs corresponding to different magnetic field strength H.

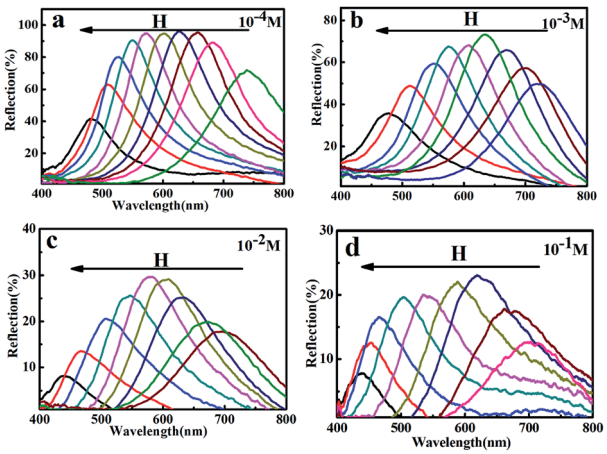

Fig. 5 (a–d) Reflection spectra of the MRPCs as NaCl concentration from 1.0×10^{-4} mol L^{-1} to 1.0×10^{-1} mol L^{-1} at pH 6.0–7.0.

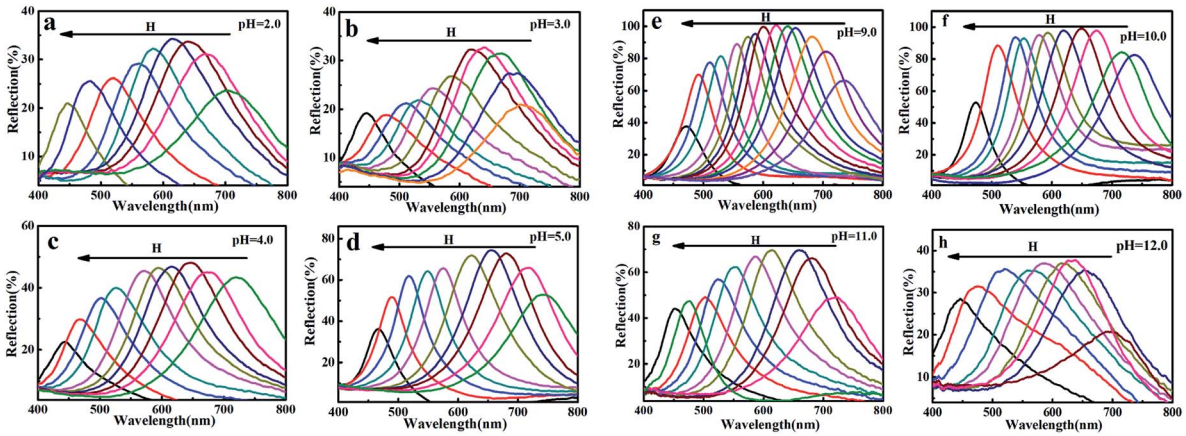

Fig. 6 (a–h) Reflection spectra of the MRPCs as pH ranged from 2.0 to 12.0, adjusted by adding different concentrations of HCl or NaOH.

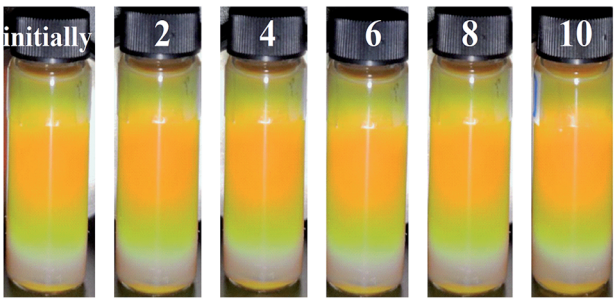

Fig. 7 Optical pictures of the MRPCs at 0.11 T after washing 2, 4, 6, 8, 10 times with deionized water.

fixed on the surface of the MCNPs owing to coordination effect between iron and PVP.

Furthermore, the MCNPs could be regenerated simply through water washing, and be reutilized. As shown in Fig. 8a, as the NaCl concentration increased, the structural color of the MRPCs blue-shifted slightly. When NaCl concentration was 1.0×10^{-1} mol L^{-1}, the structural color was bluish purple and became faded. In aqueous solution, the hydrogen bond between N on the heterocyclic pyrrole in PVP and H in water molecule made PVP chain stretching, which gave the steric hindrance to balance the magnetic attraction as magnetic assembly of MRPCs. With the increase of NaCl concentration, the hydrogen bond would be weakened, and the PVP chain would shrink. Thus, the structural color of the MRPCs would be blue-shifted. As NaCl concentration was more than 0.1 mol L^{-1}, and the structural color would be dimmed due to some particles aggregation and deposition. Since the hydrogen bond was broken severely, the PVP chain was too short to resist the magnetic attraction among the MCNPs. However, after washing with deionized water, the system could completely recover the initially structural color. Fig. 8b showed the optical pictures of the MRPCs in different pH aqueous solutions. The color blue-shifted as pH moved to acidity or alkalinity. Expectedly, as it was washed to neutral, the structural color could completely recover to its initial color. The experimental results testified the stability of the assembly coating, as well as renewable utilization of the MRPCs.

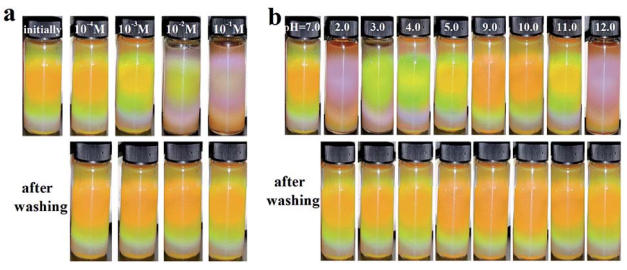

Fig. 8 (a) Optical picture of the MRPCs at different concentrations of NaCl and after washing with water, (b) optical pictures of the MRPCs in different pH systems and after washing with water.

Conclusions

In summary, the MCNPs, as the building blocks to construct MRPCs, could be prepared by the miniemulsion self-assembly of amphiphilic random copolymer with one-step process. The developed strategy to self-assemble MCNPs had the merits of simplicity, rapidity, convenience and without polymerization process. The MRPCs with bright structural color had the advantages of controllable PBG covering entire visible spectrum, salt-resistance, pH-endurance, and renewability. The present work provided a novel route to prepare MRPCs, which would greatly promote the practical application and expand the application fields.

Conflicts of interest

There are no conflicts to declare.

Acknowledgements

This research was financially supported by the Fundamental Research Funds for the Central Universities (JUSRP21937).

References

1 M. Kamenjicki, I. K. Lednev, A. Mikhonin, R. Kesavamoorthy and S. A. Asher, *Adv. Funct. Mater.*, 2003, **13**, 774–780.
2 H. Kim, J. Ge, J. Kim, S. E. Choi, H. Lee, H. Lee, W. Park, Y. Yin and S. Kuon, *Nat. Photonics*, 2009, **3**, 534–540.
3 R. Xuan and J. Ge, *Langmuir*, 2011, **27**, 5694–5699.
4 H. Hu, Q. Chen, J. Tang, X. Hu and X. Zhou, *J. Mater. Chem.*, 2012, **22**, 11048–11053.
5 Z. Cai, N. L. Smith, J. Zhang and S. A. Asher, *Anal. Chem.*, 2015, **87**, 5013–5025.
6 J. Kang, J. H. Moon, S. Lee, S. Park, S. G. Jang and S. Yang, *Adv. Mater.*, 2008, **20**, 3061–3065.
7 A. K. Bohaty and I. Zharov, *Langmuir*, 2006, **22**, 5533–5536.
8 X. Xu, S. A. Majetich and S. A. Asher, *J. Am. Chem. Soc.*, 2002, **124**, 13864–13868.
9 W. Cheng, K. Tang and J. Sheng, *Chem.–Eur. J.*, 2010, **16**, 3608–3612.
10 K. Cheng, Q. Chen, Z. Wu, M. Wang and W. Hui, *CrystEngComm*, 2011, **13**, 5394–5400.
11 J. Ge, H. Lee, L. He, J. Kim, Z. Lu and H. Kim, *J. Am. Chem. Soc.*, 2009, **131**, 15687–15694.
12 W. Cheng, K. Tang, Y. Qi, S. Jie and Z. Liu, *J. Mater. Chem.*, 2010, **20**, 1799–1805.
13 X. Xu, G. Friedman, K. D. Humfeld, S. A. Majetich and S. A. Asher, *Adv. Mater.*, 2001, **13**, 1681–1684.
14 J. Ge, Y. Hu and Y. Yin, *Angew. Chem., Int. Ed.*, 2007, **46**, 7428–7431.
15 J. Ge and Y. Yin, *Adv. Mater.*, 2008, **20**, 3485–3491.
16 W. Luo, H. Ma, F. Mou, M. Zhu, J. Yan and J. Guan, *Adv. Mater.*, 2014, **26**, 1058–1064.
17 A. You, Y. Cao and G. Cao, *Chem. Res. Chin. Univ.*, 2017, **33**, 525–529.
18 K. Landfester, *Macromol. Rapid Commun.*, 2001, **27**, 689–757.
19 F. J. Schork, Y. Luo, W. Smulders, J. P. Russum and K. Fontenot, *Adv. Polym. Sci.*, 2005, **175**, 129–255.
20 X. Liu, Y. Guan, Z. Ma and H. Liu, *Langmuir*, 2004, **20**, 10278–10282.
21 A. Khan, A. M. El-Toni, M. Alsalhi, A. S. Aldwayyan and M. Alhoshan, *Mater. Lett.*, 2012, **76**, 141–143.
22 F. Tiarks, K. Landfester and M. Antonietti, *Langmuir*, 2001, **17**, 908–918.
23 L. Zhu, X. Yang and Y. Cao, *Anal. Lett.*, 2013, **46**, 982–998.
24 L. He, M. Wang, J. Ge and Y. Yin, *Acc. Chem. Res.*, 2012, **45**, 1431–1440.
25 E. Murugan, J. N. Jebaranjitham, M. Ariraman, S. Rajendran, J. Kathirvel, C. R. Akshata and K. Kumar, *ACS Omega*, 2018, **3**, 13685–13693.
26 B. Liu, W. Zhang, F. Yang, H. Feng and X. Yang, *J. Phys. Chem. C*, 2011, **115**, 15875–15884.
27 G. Beamson and D. Briggs, *High Resolution XPS of Organic Polymers: The Scienta ESCA300 Database*, John Wiley & Sons, Chichester, England & UK, 1992.
28 W. Wei, W. Ye, J. Wang, C. Huang, J. B. Xiong, H. Qiao, S. Cui, W. Chen, L. Mi and P. Yan, *ACS Appl. Mater. Interfaces*, 2019, **11**, 32269–32281.
29 W. Wei, W. Chen, L. Ding, S. Cui and L. Mi, *Nano Res.*, 2017, **10**, 3726–3742.
30 S. A. Krasnikov, A. S. Vinogradov, K. H. Hallmeier, R. Höhne, M. Ziese and P. Esquinazi, *J. Mater. Sci. Eng. B*, 2004, **109**, 207–212.
31 H. Y. Lee, N. H. Lim, J. A. Seo, S. H. Yuk, B. K. Kwak and G. Khang, *J. Biomed. Mater. Res., Part B*, 2010, **79**, 142–150.
32 L. Wang, L. Jin, F. Quan, M. Suzuki, I. S. Suzuki and M. H. Engelhard, *J. Phys. Chem. B*, 2005, **109**, 21593–21601.
33 X. Teng, D. Black, N. J. Watkins, Y. Gao and H. Yang, *Nano Lett.*, 2003, **3**, 261–264.
34 D. Wilson and M. A. Langell, *Appl. Surf. Sci.*, 2014, **303**, 6–13.
35 S. Poulin, R. França, L. Moreaubélanger and E. Sacher, *J. Phys. Chem. C*, 2010, **114**, 10711–10718.
36 X. Xu, G. Friedman, K. D. Humfeld, S. A. Majetich and S. A. Asher, *Chem. Mater.*, 2002, **14**, 1249–1256.
37 J. Ge, L. He, Y. Hu and Y. Yin, *Nanoscale*, 2011, **3**, 177–183.
38 H. Hu, C. Chen and Q. Chen, *J. Mater. Chem. C*, 2013, **1**, 6013–6030.
39 D. H. Everett, *Basic Principles of Colloid Science*, The Royal Society of Chemistry, London, 1988.